ERJ Express. Published on September 5, 2007 as doi: 10.1183/09031936.00000507

REVISED MANUSCRIPT

Three-Dimensional CT Imaging in an Animal Model of Emphysema

Aaron R Froese[1], Kjetil Ask[1], Renee Labiris[2], Troy Farncombe[3], David Warburton[4], Mark D Inman[2], Jack Gauldie[1], Martin Kolb[1,2]

[1] Department of Pathology and Molecular Medicine, Center for Gene Therapeutics, McMaster University, Hamilton, Ontario, Canada

[2] Department of Medicine, Firestone Institute for Respiratory Health, McMaster University, Hamilton, Ontario, Canada

[3] Department of Nuclear Medicine, Hamilton Health Sciences, McMaster University, Hamilton, Ontario, Canada

[4] Developmental Biology Program, Saban Research Institute, Children's Hospital Los Angeles, University of Southern California

Corresponding address:
Dr. Martin Kolb, MD, PhD
Departments of Medicine, Pathology and Molecular Medicine
McMaster University
Firestone Institute for Respiratory Health
50 Charlton Ave East, Room T2121
Hamilton, Ontario, Canada L8N 4A6
Ph. (905) 522.1155 ext 4973
Fax (905) 521.6183
e-mail: kolbm@mcmaster.ca

Funded by: Canadian Institute for Health Research
Key words: animal model, computed tomography, emphysema, non-invasive assessment,
Word Count: 3640

ABSTRACT

Emphysema is a major health problem and novel drugs are needed. Animal disease models are pivotal in their development, but validity and sensitivity of current tools to evaluate drug efficacy are limited. We investigated the usefulness of micro computed tomography (CT) as an innovative tool to assess emphysema in a mouse model.

Serial CT was performed in two-weekly intervals in Smad 3 knockout (KO) mice, which spontaneously develop airspace enlargement. Lung density was quantified in 2D and 3D images and correlated to mean linear intercept and lung compliance.

CT-scans of Smad3 KO lungs revealed a significant decrease in lung density at 8 weeks age and progression towards 14 weeks with respect to age matched wildtype (WT) animals. Emphysema could be reliably assessed with both the 2D and 3D approach, but 3D was superior due to normalization to lung volumes and less variability. Lung compliance by week 14 was 0.053 +/- 0.005 and 0.034 +/- 0.002 % max vol/cmH_2O for KO and WT mice ($p<0.007$), reflecting physiologically relevant emphysema.

Conclusions: Small animal CT-imaging and density quantification in a reconstructed 3D image is a useful tool to quantify emphysematous changes in an animal disease model. It adds significant information to conventional assessment.

INTRODUCTION

COPD and emphysema are recognized as major global health problems. The defining feature of COPD is irreversible airflow obstruction, caused by elevated resistance in the small airways and increased lung compliance due to emphysema and lung destruction (1)(2). The pathogenesis of COPD involves repeated and/or persistent injury to the lung caused by noxious particles and gases, which lead to chronic inflammation with oxidative stress and high protease activity (3)(4). The exact mechanism of progression from tissue injury to irreversible damage in airways and parenchyma is not completely understood (5)(6). One prevailing hypothesis for the development of emphysema involves a protease – anti-protease imbalance favoring a "matrix degrading micro-environment" in the lungs (7).

Animal models have substantially broadened our knowledge of the development of emphysema and are instrumental to identify novel treatment targets (8). The most common approach to an experimental model of emphysema is the intratracheal instillation of elastase, which causes rapid and progressive emphysema. Cigarette smoke exposure also leads to emphysema in animals, but requires relatively long times to develop. There are a number of genetically altered animals, such as mice null for the Smad 3 gene, which lack an integral signaling molecule in the transforming growth factor (TGF) β pathway and develop age related enlargement of the alveolar airspace (9). Airspace enlargement develops slowly and relatively more homogeneous in the Smad3 KO mice with absence of emphysematous bullae (see Figure 1), while it is patchier in the smoking and even more in the elastase model. Due to feasibility, drug efficacy experiments are most often done in the elastase model (8). For this purpose emphysema

is usually evaluated by morphometry, e.g. measuring mean linear intercept (MLI), or perhaps quantifying matrix gene expression and protein concentration. This approach seems to be fairly simple and fast, and can provide proof of principle if applied appropriately. However, morphometric techniques are not always used correctly and can be misinterpreted. Fehrenbach recently reviewed the literature and noted that careful inspection of many of the animal models revealed that strict criteria of emphysema definition were demonstrated in surprisingly few of them (10). Further, the applicability of the findings to a human disease, which requires decades to develop, remains questionable. The current assessment tools cannot be repeated to follow a single animal, and may display artifacts of fixation and inflation not relevant to actual lung architecture or function.

The progressive destruction of alveoli in emphysema leads to a loss of gas exchange surface resulting in a decrease of lung parenchyma density. This structural change can be quantified in the human by a computed tomography X-ray scanner (11)(12). Although pulmonary function tests are the conventional method for diagnosis and clinical management of COPD and emphysema, they have weaknesses (13)(14). CT imaging can give useful information for the diagnosis of emphysema in humans today which may even be superior to functional assessment (12). The value of quantitative CT seems to be even stronger in assessing small changes in the lung parenchyma of human patients and may allow the visualization of the progression of disease or quantify changes due to interventions (15)(16). Micro-CT may have similar potential in assessing emphysematous changes in animal models of disease.

Here we validate micro-CT scans as a new method for evaluating disease progression in an animal model of emphysema. We show that micro-CT correlates with both MLI in 2D and lung function in Smad3 KO mice (17)(18). This study is the first to validate 2D and 3D micro-CT imaging in a mouse model of progressive airspace enlargement.

METHODS

Animals Care

All mice were treated in accordance with the guidelines of the Canadian Council of Animal Care. All animal procedures were performed under inhalation anesthesia with isofluorane (MTC Pharmaceuticals, Cambridge, ON) or Avertin (Aldrich Chemical Co., Milwaukee, WI) without giving supplemental oxygen. Exon 8 of the Smad3 gene was disrupted in mice with background 129SV/EV x C57BL/6 (18). Mice were bred in special pathogen-free rooms.

Histology

For histological examination, lungs were inflated and fixed by intratracheal instillation of 10% neutral buffered formalin at a constant pressure of 20 cm of water for 5 minutes. After fixation in 10% buffered formalin for 24 hours, lungs were paraffin embedded, cut in 3um sections, and stained with hematoxylin & eosin.

CT Scanning

Spontaneously breathing mice were imaged under isoflurane anesthesia using the CT portion of an X-SPECT SPECT/CT (Gamma Medica-Ideas, Northridge, CA). The x-ray tube was set to 80 kVp and 220 μA. Image acquisition was performed using a continuous rotation, acquiring 512 projection measurements into a 1024x1024 array (0.10 mm pixel size). Images were reconstructed using a Feldkamp cone beam reconstruction algorithm into 512x512x512 arrays (0.1157 mm voxels), and then rescaled to provide CT

numbers. Whole body X-ray dosimetry was measured using TLD 100 chips (Harshaw-Thermo RMP, Solen, OH) embedded in six places in the body of dead mice and exposures averaged. The chips were read by (Global Dosimetry Solution Inc., Irvine, CA). Mice scanned for 120 seconds yielded an average whole body exposure of approximately 27 mGy. Reconstructed image data was then analyzed using Amira® software (Mercury Computer Systems, Chelmsford, MA) to quantify lung tissue density. 3D volumes were drawn manually around the anatomical lungs in each image. Lung tissue density within these volumes were determined by constructing a histogram over the CT number range from -1000 to -100 using 18 bins of width 50 Hounsfield Units (HU). CT numbers were expressed as averages of the percentage of total lung volume for a given group.

Validation experiments were performed to demonstrate that our imaging approach was able to reliably detect changes in densities of lung inflated with different volumes of air. Naïve Balb/c mice (n=5) underwent the imaging protocol in four different conditions: spontaneously breathing under isofluorane anaesthesia, dead with open trachea, dead with trachea blocked and lungs inflated with 500 μL and 700 μL air.

2D Morphometry to 2D CT Density Correlation

Trans-axial histological sections from eight animals (4 KO, 4 WT) were highlighted in select areas of airspace enlargement and normal lung tissue. MLI measurements were taken manually by counting the intercepts with 10 randomly placed lines on each of at least 7 photographs per highlighted area. The closest 2D trans-axial CT slice was highlighted in the same selected areas and analyzed for voxel count and

density. The voxels with density between -550 and -450 HU were summed and analyzed against the same area's MLI. These densities were selected because they correspond to normal (-450HU) and enlarged airspaces (-550 HU).

Pressure Volume Loop Determination

All pressure volume loops were performed with a quantitative mechanical respirator (flexiVent, SCIREQ Scientific Respiratory Equipment, Montreal, QC). In order to avoid possible bronchodilatory effects of Isoflurane, animals were anesthetized with Avertin (Aldrich Chemical Co., Milwaukee, WI) at 240 mg/Kg IP and paralyzed with Pancuronium bromide (Sandoz Canada Inc., Boucherville, QC) 0.03mg/kg IV. An intratracheal tube was then inserted and the animal placed on mechanical ventilation. The positive end expiratory pressure was constant at 2 cmH20.

Statistical analysis

Data are shown as mean +/- SEM. For evaluation of differences between Smad 3 KO and WT group values, we used student's t test. ANOVA (F-test) was used in evaluating the variability between individual analyzers during the inflated-mouse CT validation. P values less than 0.05 were considered significant. Linear regression was used for the comparison of two variables sets.

RESULTS

Smad 3 KO emphysematous progression

We have previously described the progression of airspace enlargement in Smad 3 mice to be spontaneously acquired with age (9). Figure 1 illustrates the extent of airspace enlargement seen in KO animals up to 14 weeks of age whereas WT animals are essentially unchanged. Enlargements in MLI for KO animals are significant at 8 weeks, and increase further to 14 weeks of age.

2D Morphometric Correlation to CT Density

The histomorphology from animals with and without airspace enlargement were correlated with the same 2D slice from concurrent CT scans. Areas with obvious emphysema and normal lung parenchyma were photographed and analyzed for MLI (Figure 2A). The same area in the 2D trans-axial slice was analyzed for the amount of lower density voxels between –450 and –550 HU as only these selected voxels showed correlation with MLI data. Figure 2A shows for example that area A1 has significantly more airspace enlargement and lower CT densities than area B1. Furthermore, the increasing low density seen in the CT scan correlated with severity of airspace enlargement seen in the histology. There was significant visible correlation between areas with normal and low density in the 2D CT slice and the position of normal and emphysematous regions in the histology. Areas that contained visible airspace enlargement in the histology correlated with scan densities of approximately -550 HU

and below. Figure 2B shows the correlation between 2D areas in the CT image summed from -550 to – 450 HU and the same area's MLI for 16 areas (R^2=0.53).

Computed Tomography – 3D Density Analysis

Conventional research of emphysema in animal models relies on mean chordal length measurements taken from random areas of the lung and then averaged. This analysis is usually performed on a single section of lung thereby missing potential patchy areas of airspace enlargement. Similar limitations may apply to 2D CT imaging. In contrast, 3D CT images can be used to find the spatial orientation and density of mouse lungs with time. Spatial orientation of low density voxels may vary between subjects but the amount of low density voxels can be averaged from three dimensional images to find significance between groups. Voxels with density of -550 to -1000 HU were considered to represent emphysematous changes since these densities were not seen in the normal lungs of WT animals. Figure 3 A to C show Smad 3 knockout and wild type mice which have been serial scanned from 6 weeks to 14 weeks of age. As the mice progress in age, a shift toward less dense tissue can be visualized. The Smad 3 mouse is fairly heterogeneous with some knockout animals displaying more low-density tissue than others. Smad 3 KO mice do not all progress to emphysema at the same age, but in general, increases in MLI and low-density voxels were observed at the onset of sexual maturation (about 6-7 weeks). Images were reconstructed in 3D to help visualize changes in MLI in the lungs of KO animals over time. Figure 3 D shows images from one representative knockout and wildtype mouse in which amounts of low density tissue, colored yellow (-700 HU to -550 HU), increase greatly from 6 to 14 weeks. The finding

that 2D transaxial slices correlated well with 3D densities is supported by the even distribution of airspace enlargement throughout the Smad3 KO lung.

2D and 3D Computed Tomography Data Compared

In the past, 2D slices were analyzed to determine differences between groups. The weight was on the radiologist to find the best representative slice for the whole lung. To ascertain if the amounts of low density tissue seen in Smad 3 KO were also found in WT animals, 2D slices were extracted from the top and bottom of each CT scan. As expected, the data revealed differences in amount of low density voxels between -1000 to -550 HU. Figure 4A shows the percentage of whole 2D slices with densities between -1000 to -550 HU. With age, the KO 2D slice voxels decrease in density and are significant at 10 and 14 weeks of age with respect to WT age matched animals ($p < 0.01$ and $p < 0.05$ respectively). The density of KO lungs on average were decreased at 14 weeks with respect to KO animals at 6 weeks of age ($p < 0.04$). In comparing data extracted from the 2D slices to 3D whole lungs, we found high correlation between the two ($R^2 = 0.94$), suggesting that the densities from two averaged 2D slices were representative of densities in the whole scan in this model. However, despite the homogeneous pattern of airspace enlargement in Smad3 KO mice, 3D data had less variability (CV= 1.43) compared with 2D variability (CV=1.24). The difference in summed low density voxels of KO lung to controls achieved higher levels of significance in 3D compared to 2D analysis ($p=0.00007$ vs. $p=0.0005$). It can be anticipated that the variability would be markedly increased in a model with patchier tissue changes (Figure 4B and C).

Validation of Lung Density Analysis

Validation experiments were performed to demonstrate the validity of our imaging method in detection of changes in lung densities. Naïve Balb/c mice (n=5) underwent the imaging protocol in four different conditions: spontaneously breathing, dead with open trachea, dead with trachea blocked and lungs inflated with 500 μL and 700 μL air. The mean lung volume of spontaneous breathing mice weighing 20-30 g was 619 μL ± 63.4 with a maximum voxel count at densities between -425 and -375 HU. After euthanization, the mean lung volume was 352 μL ± 20.2 with a maximum voxel count at densities between -375 and -325 HU. With inflation of the lung with known air volumes, a change in lung volume calculated from the CT scan was 485 μL ±47 after instillation of 500 μL and 748 μL ±27 after 700 μL (Figure 5). Note that traditional human emphysematous CT densities in the area of -950 HU are never reached by over-inflated mice. The quantitative analysis of the CT images was performed independently by 3 different raters. The total lung volume was determined by each analyzer and averaged for each mouse. Using the F-test, there was insufficient evidence to conclude that there was a difference between analyzers with a 98% confidence interval. We performed one additional experiment on one mouse that was imaged at 8 different times to determine repeatability of the measurements. The coefficient of variation of total lung volume among the 8 scans was 7.7%. These results confirm that calculation of lung volume from the CT image was sensitive to changes in air volume, repeatable and has a high inter-rater reliability.

Physiological Correlation – Pressure Volume Loop

Pressure volume loops were measured ex vivo to determine whether or not the changes seen in the CT density figures actually represented physiological differences in lung compliance. Figure 6A shows the average quasi static pressure volume loop of knockout and wildtype animals. Figure 6B illustrates that at 14 weeks of age the Smad 3 KO mice show a marked increase in compliance compared to the WT controls ($p<0.007$).

DISCUSSION

Animal models of emphysema are pivotal in identifying and evaluating novel therapeutic interventions in this disease. The current approaches to assess drug efficacy in emphysema models have limitations and the transferability to human disease remains questionable. Here we show data representing the attempt to use CT imaging as a method to follow the progression of emphysema in a mouse model using 2D and 3D quantitative analysis over time. The highlights of this method are that it is reliable, fast and diagnostic of emphysema-like changes. It further has the advantage of longitudinal follow up of individual animals and avoids problems associated with fixation artifacts and morphometry.

Our knowledge of the molecular mechanisms involved in emphysema development steadily increases, substantially assisted by animal disease models (8). Intratracheal instillation of noxious hazards such as elastase or cigarette smoke exposure can cause emphysema. Similarly, emphysema develops spontaneously in naturally occurring mutant mouse strains or in genetically altered animals. Novel molecular targets have been identified, and drugs are being developed to interfere with molecular mechanism of emphysema. Due to time constraints and feasibility, drug efficacy experiments are usually done in the elastase model (8) which provides early endpoints and a rapid read out. Emphysema is currently evaluated by histomorphometry, and reliable determination of mean linear intercept or chordal length requires careful and standardized inflation of the lungs. Any leak in the airways or on the pleural surface would result in incorrect measurements (19). The lung images shown in Figures 1 and 2

were purposely obtained at low magnification to illustrate that even with a validated method using standardized inflation pressure to prepare tissue slides for histomorphometry does not always result in pictures that are shown in textbooks.

Here we show that CT imaging in animal models of emphysema is not only able to provide reliable quantification of air space enlargement similar to histomorphometry, but has several advantages over the conventional methods. Non-invasive CT scanning does not require euthanasia and can be performed as needed at several time points. It also can be repeated in individual animals to visualize a dynamic disease progression, or reversibility in case of drug efficacy studies. This does not only help to account for inter-individual variability, but also reduces the number of animals required for a study.

The current technique was chosen due to its short image acquisition time and being the lowest dose of radiation required for detection of emphysematous progression. Acquisition of data is swift, requiring only 2 minutes per scan. The data can be then reconstructed in another 2 minutes and further analyzed for 3D assessment using Amira Imaging Software in another 5 minutes. We determined that the radiation dose of a 120 second scan is approximately 27 mGy, some 50 times less than values capable of significant lung damage (20). The resolution of the scans is 115 mm^3, which - although large compared to the finest micro-CT resolutions - shows significant and meaningful differences between animals with and without emphysema. It is noteworthy that the animals in our study were under general anesthesia but spontaneously breathing, thus each animal was analyzed at a volume close to its FRC, which may well have changed between groups, based on our observed differences in the pressure volume loops. Had we chosen to ventilate the animals, we would have introduced the problem of changing the

lung volume depending on the ventilator frequency (21). We consider these measurements as evidence of functional emphysema in the Smad 3 KO mice. For histological analysis, mouse lungs were inflated to 20 cmH_2O and formalin fixated. This was performed as a means to standardize all lungs to a fixed point on their pressure volume relationship prior to analyzing for evidence of airspace enlargement. Given that there were obviously differences in lung volumes at the time of functional and histological assessment, any direct comparisons in terms of airspace size between these conditions would not be appropriate. Using these independent methods, we show that Smad 3 KO mice develop airspace enlargement over time, and demonstrate in follow up studies of individual mice that these emphysema like changes correlate significantly with 2D morphometry. We further show that the loss of lung parenchyma as assessed by decrease in density in the 3D image is associated with increased compliance of the lungs, strengthening the validity of the imaging technique as a meaningful outcome for assessment of an animal model of emphysema.

Why 3D?

The most common form of emphysema is smoking related and develops from enlarged terminal bronchioli, progressing in a centrilobular pattern. The lung apices are usually more involved than the bases. Panacinar emphysema typically is associated with alpha-1-antitrypsin deficiency and is more present in the bases, overall more uniform than the patchier distribution of the former (1). Data from older studies suggest that one or the other of these emphysema types usually dominates in advanced disease (22), emphasizing that emphysema develops in a heterogeneous manner and that single slice

histomorphometry at a single time point may not suffice to obtain reliable data. Further, it is well known that only about 15 % of smokers develop clinically symptomatic COPD whereas 40 % show signs of emphysema (23), suggesting a long subclinical course of emphysema. Emphysema in animal disease models can progress in a similar patchy pattern from a centriacinar lesion, depending on the initiating agent and species of animal used in the experiment (24). To date, most imaging related questions asked in animal models of emphysema have relied on 2D CT slices. The patchy pattern of emphysema may be lost in histomorphology or 2D imaging, but not using a 3D approach (25). The Smad 3 KO model described herein seems to have slightly more airspace enlargement in the central areas of the lungs, but the decreases in density are fairly evenly present toward the top and bottom of the lung. Although 2D and 3D image analysis correlated significantly in our study, we still found a high variability in lung density assessed by 2D slice analysis compared to the 3D approach. It can be anticipated that the variability of 2D data will be markedly higher in a model with patchier emphysema, such as the elastase model, which is commonly used for drug efficacy experiments. Furthermore, any technique involving slices of a three dimensional structure may imply some bias on the part of the investigator during the attempt to find the most representative slices. Finally, 3D but not 2D based analysis of lung density is adjusted to lung volume. Air trapping, a dynamic hyperinflation of the lungs but not structural emphysema, would appear as area with low density in a 2D image and as such labeled as emphysema, whereas in 3D image analysis, it would be related to lung volume and not be considered emphysema. In addition, 3D image analysis is substantially faster that 2D with the availability of appropriate software. All this makes 3-dimensional reconstruction of the CT image and

quantification of lung density a powerful tool which seems to be more efficient than conventional 2D assessment.

In summary, we have demonstrated that CT imaging and density quantification in a reconstructed 3D image is a useful tool to quantify emphysema like changes in an animal disease model. It is at least as reliable as conventional histomorphometry, but has the advantage that individual animals can be followed over time. The method is fast, easy to perform and cost efficient. We believe that his assessment tool will be extremely valuable in drug efficacy experiments in emphysema research.

ACKNOWLEDGEMENTS

We acknowledge the expert technical assistance of Russ Ellis, Carol Lavery, Tanzeel Rahman, Chantal Saab and Jennifer Wattie. Dr. Doug Boreham for performing radiation dosimetry. R.L. is a recipient of the Father Sean O'Sullivan Career Award. M.K. is supported by a career award from the Department of Medicine at McMaster University. Grant support through Canadian Institute for Health Research.

LEGENDS

Figure 1. Smad3 Null Mice, a model of airspace enlargement. (A) Smad 3 KO mice develop emphysema spontaneously with age. Representative histology pictures of a KO and WT mouse at 14 weeks of age. (B) Whole lung voxel counts illustrating lung size. Lines illustrate averages and (*) denotes $p < 0.001$ with respect to 6 Week WT data and (**) denotes $p < 0.004$ with respect to age matched WT.

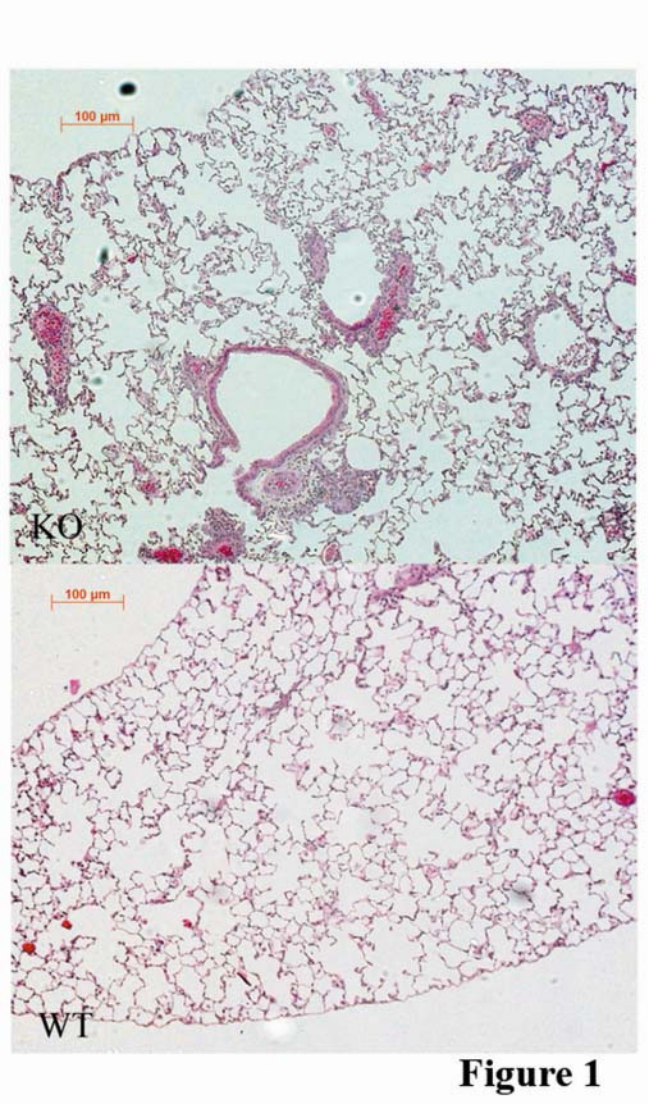

Figure 1

Figure 2. Histomorphometric correlation with 2D CT densities. (A) Comparison of airspace enlargement for correlation between histomorphology and increases in low-density voxels in 2D CT slices. The histology was analyzed for mean linear intercept (MLI) in areas of airspace enlargement and normal areas. Trans-axial CT slices were chosen to be as close as possible to the same trans-axial slice in the histology. The same regions in the 2D CT slice were extracted and density histograms created. Voxels with densities between –550 and –450 HU were summed as only these densities correlated with MLI. Red represents -600 to -700 HU, yellow represents -600 to -550 HU, and blue represents -550 to -100 HU. All mice analyzed were 14 weeks of age. (B) Correlation of summed 2D CT slice voxel densities with 2D morphometry. Number of areas analyzed was 16 from 8 animals (4 KO, 4 WT). Correlation of morphology to CT densities had an R^2 of 0.53.

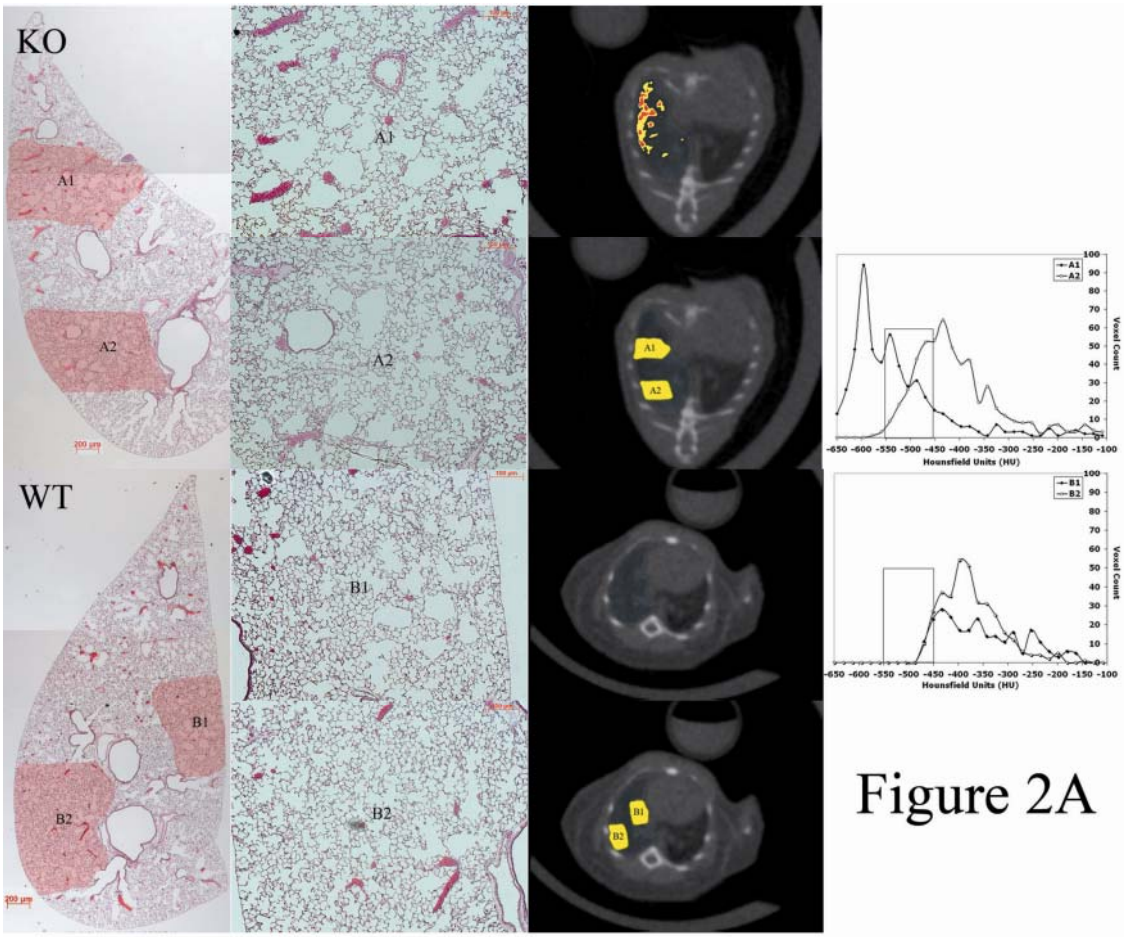

Figure 2A

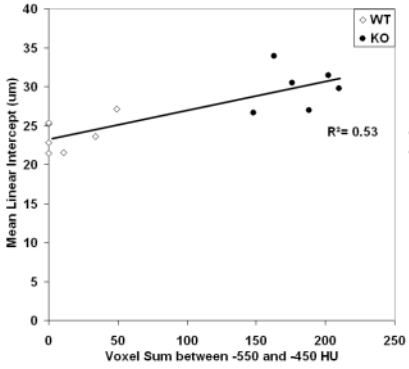

Figure 2B

Figure 3. Progression of Smad3 KO airspace enlargement with age. (A) Average percent of total lung volume at time of scan at 6 weeks (n=4 KO, n=6 WT), (B) 10 weeks (n=8 KO, n=11 WT) and (C) 14 weeks (n=9 KO, n=15 WT). (D) 3D images displaying

decreased lung density with time. Images are of a representative Smad 3 KO (top) and WT (bottom) mouse from 6 through 14 weeks of age. Yellow color coding represents voxels with densities between -700 and -550 HU, blue represents -550 to -100 HU.

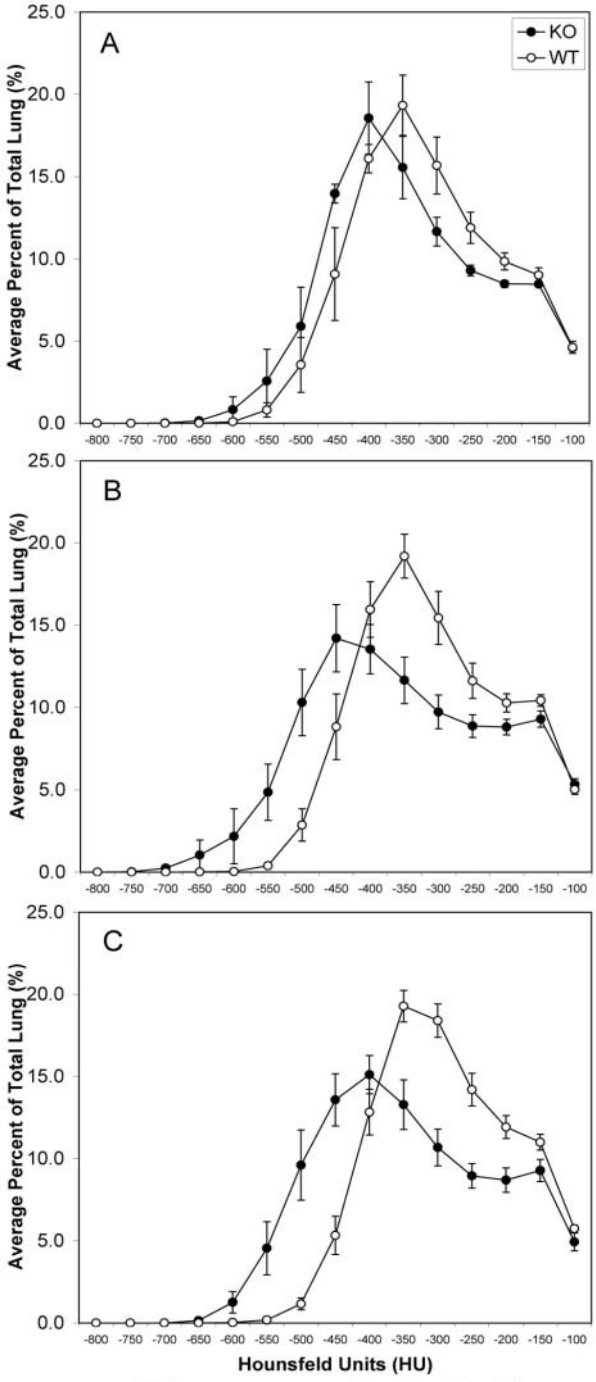
A
B
C
KO
WT
Average Percent of Total Lung (%)
25.0
20.0
15.0
10.0
5.0
0.0
-800 -750 -700 -650 -600 -550 -500 -450 -400 -350 -300 -250 -200 -150 -100
Hounsfeld Units (HU)

Figure 3 ABC

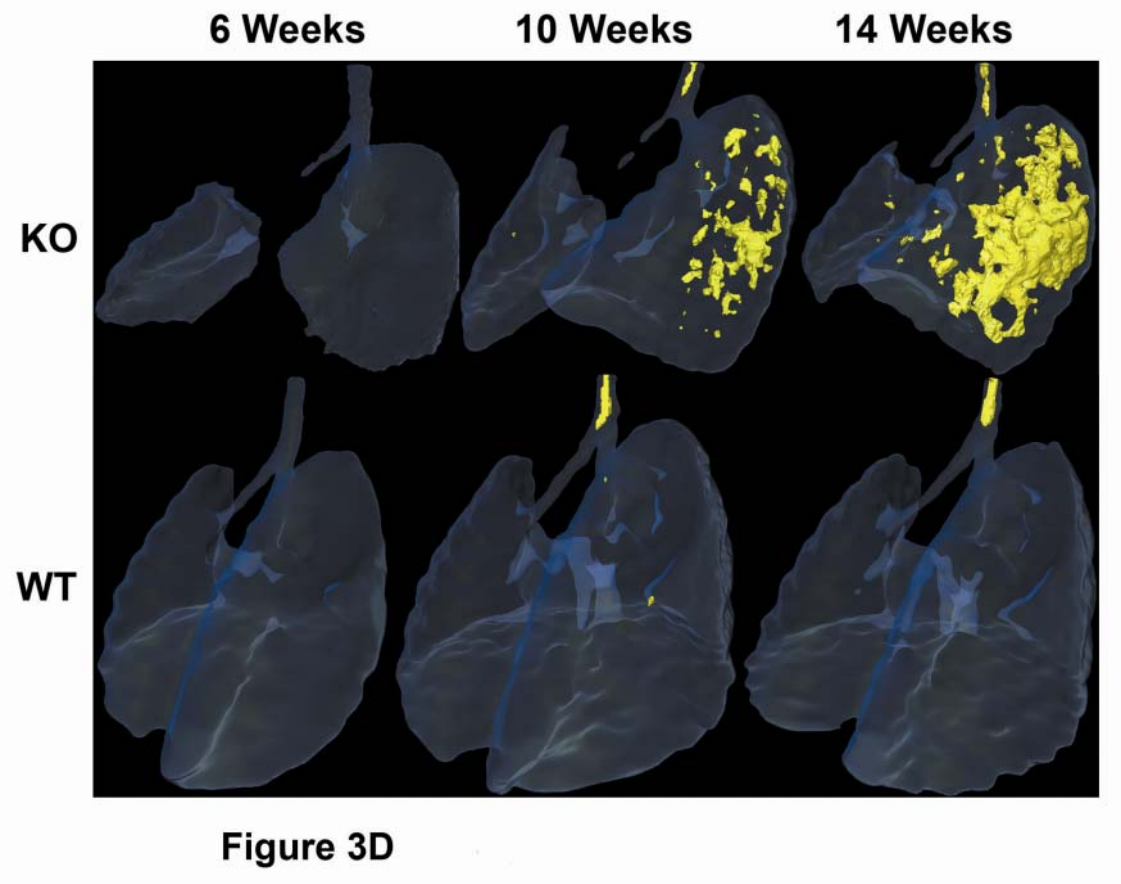

Figure 4. Correlation of 2D to 3D CT densities. (A) Average percentage of whole 2D slices with densities between -1000 to -550HU. Two slices were extracted per scan. The top slice was always 32 slices under the top of the lung and the bottoms slice was always taken 32 slices above the bottom of the lung. (*) denotes $p < 0.01$ with respect to age matched WT and (**) denotes $p < 0.04$ with respect to 6 or 8 week KO. (B) Average percentage of whole 3D lung with densities between -1000 to -550HU. (*) denotes $p < 0.01$ with respect to age matched WT. (**) denotes $p < 0.006$ with respect to KO at 6 or 8 weeks. (***) denotes $p < 0.001$ with respect to KO at 6 weeks of age. (C) Correlation of 2D and 3D density data. The percentage of total 2D slice with density between -1000 and -550HU (low density) were averaged between the top and bottom of the lung. The

3D percentage of low density in the whole lung was compared against the same scan's 2D slice average with a correlation of $R^2 = 0.94$. 6 weeks (n=4 KO, n=6 WT), 10 weeks (n=8 KO, n=11 WT) and 14 weeks (n=9 KO, n=15 WT).

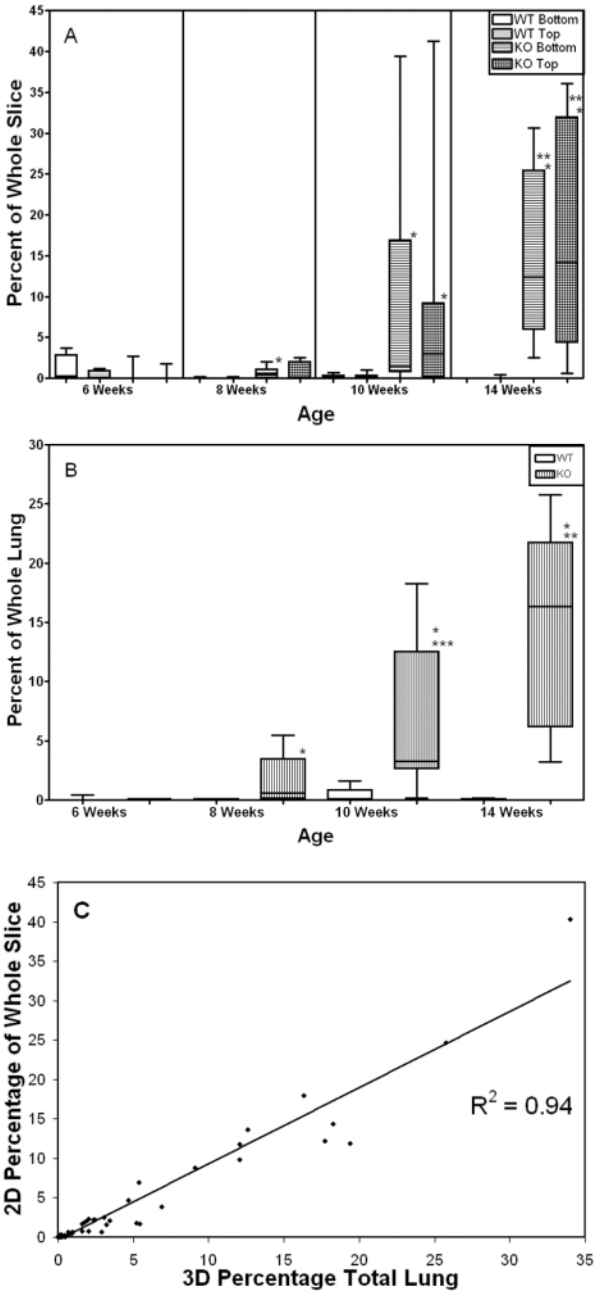

Figure 4 ABC

Figure 5. Validation of inflated lung volumes to CT densities. Average percentage of total lung volumes for mice scanned alive (n=5), dead with open trachea (n=5), dead with trachea closed and either 500uL (n=5) or 700uL (n=3) of air injected.

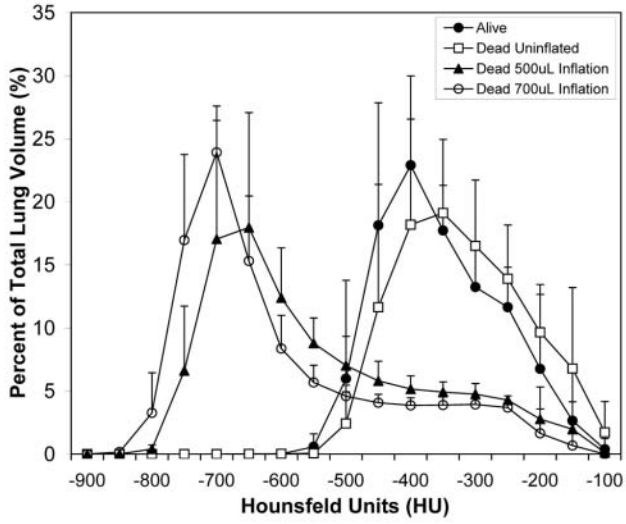

Figure 5

Figure 6. Physiological properties of Smad3 lungs. (A) Average quasi-static pressure volume loop of Smad 3 KO and WT mice at 14 weeks of age (n=8 KO, n=15 WT). (B) Significant difference in lung compliance between Smad 3 KO and WT mice ($p<0.007$). Compliance was measured by the slope of the last 8 points of the lower line of the average pressure volume loop at 14 weeks of age.

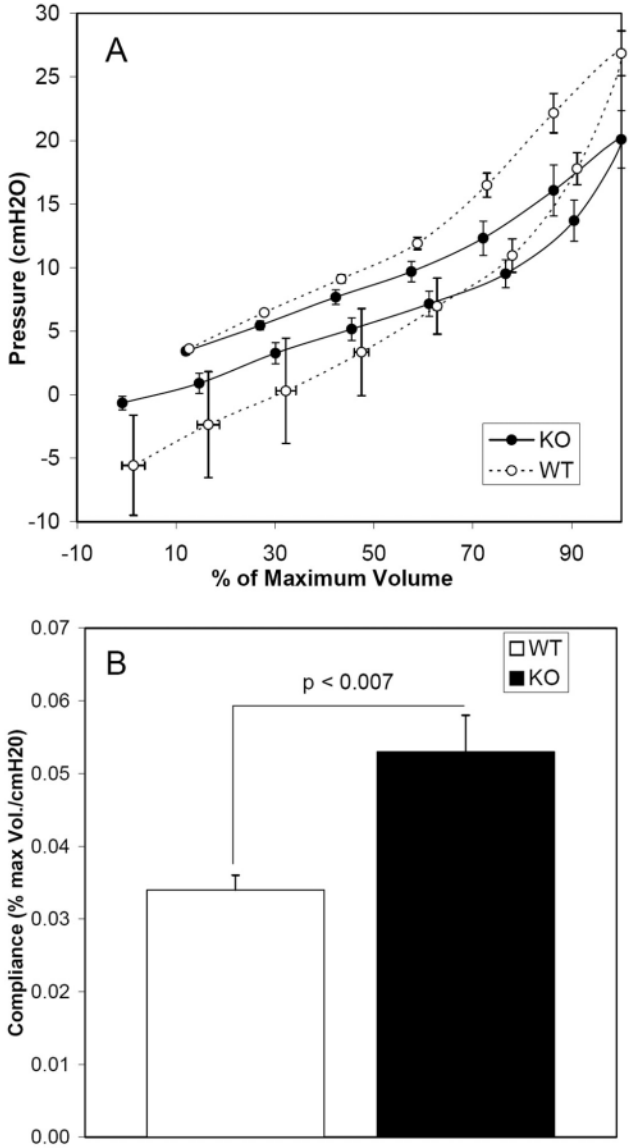
A
Pressure (cmH2O)
% of Maximum Volume
KO
WT
B
WT
KO
p < 0.007
Compliance (% max Vol./cmH20)

Figure 6

References

1. Hogg JC. Pathophysiology of airflow limitation in chronic obstructive pulmonary disease. Lancet. 2004 Aug 21-27;364(9435):709-21.
2. Keller CA. Pathophysiology and classification of emphysema. Chest Surg Clin N Am. 2003 Nov;13(4):589-613.
3. Sethi JM, Rochester CL. Smoking and chronic obstructive pulmonary disease. Clin Chest Med. 2000 Mar;21(1):67-86, viii.
4. MacNee W. Pathogenesis of chronic obstructive pulmonary disease. Proc Am Thorac Soc. 2005;2(4):258-66; discussion 90-1.
5. Churg A, Wright JL. Proteases and emphysema. Curr Opin Pulm Med. 2005 Mar;11(2):153-9.
6. Coakley RJ, Taggart C, O'Neill S, McElvaney NG. Alpha1-antitrypsin deficiency: biological answers to clinical questions. Am J Med Sci. 2001 Jan;321(1):33-41.
7. Ohnishi K, Takagi M, Kurokawa Y, Satomi S, Konttinen YT. Matrix metalloproteinase-mediated extracellular matrix protein degradation in human pulmonary emphysema. Lab Invest. 1998 Sep;78(9):1077-87.
8. Mahadeva R, Shapiro SD. Chronic obstructive pulmonary disease: Experimental animal models of pulmonary emphysema. Thorax. 2002 Oct;57(10):908-14.
9. Bonniaud P, Kolb M, Galt T, Robertson J, Robbins C, Stampfli M, et al. Smad3 null mice develop airspace enlargement and are resistant to TGF-beta-mediated pulmonary fibrosis. J Immunol. 2004 Aug 1;173(3):2099-108.
10. Fehrenbach H. Animal models of pulmonary emphysema: a stereologist's perspective. European Respiratory Review. 2006, 2006;15(101):136-47.
11. Muller NL, Coxson H. Chronic obstructive pulmonary disease. 4: imaging the lungs in patients with chronic obstructive pulmonary disease. Thorax. 2002 Nov;57(11):982-5.
12. Coxson H, Rogers R. Quantitative computed tomography of chronic obstructive pulmonary disease. Acad Radiol. 2005 Nov;12(11):1457-63.
13. Rennard SI. Chronic obstructive pulmonary disease: linking outcomes and pathobiology of disease modification. Proc Am Thorac Soc. 2006 May;3(3):276-80.
14. Uppaluri R, Mitsa T, Sonka M, Hoffman EA, McLennan G. Quantification of pulmonary emphysema from lung computed tomography images. Am J Respir Crit Care Med. 1997 Jul;156(1):248-54.
15. Stolk J, Versteegh MI, Montenij LJ, Bakker ME, Grebski E, Tutic M, et al. Densitometry for assessment of effect of lung volume reduction surgery for emphysema. Eur Respir J. 2007 Jun;29(6):1138-43.
16. Coxson HO. Computed tomography and monitoring of emphysema. Eur Respir J. 2007 Jun;29(6):1075-7.
17. Harris R. Pressure-volume curves of the respiratory system. Respir Care. 2005 Jan;50(1):78-98; discussion -9.
18. Yang X, Letterio JJ, Lechleider RJ, Chen L, Hayman R, Gu H, et al. Targeted disruption of SMAD3 results in impaired mucosal immunity and diminished T cell responsiveness to TGF-beta. Embo J. 1999 Mar 1;18(5):1280-91.

19. Parameswaran H, Majumdar A, Ito S, Alencar AM, Suki B. Quantitative characterization of airspace enlargement in emphysema. J Appl Physiol. 2006 Jan;100(1):186-93.
20. Coggle JE, Lambert BE, Moores SR. Radiation effects in the lung. Environ Health Perspect. 1986 Dec;70:261-91.
21. Volgyesi GA, Tremblay LN, Webster P, Zamel N, Slutsky AS. A new ventilator for monitoring lung mechanics in small animals. J Appl Physiol. 2000 Aug;89(2):413-21.
22. Kim WD, Eidelman DH, Izquierdo JL, Ghezzo H, Saetta MP, Cosio MG. Centrilobular and panlobular emphysema in smokers. Two distinct morphologic and functional entities. Am Rev Respir Dis. 1991 Dec;144(6):1385-90.
23. Hogg JC, Wright JL, Wiggs BR, Coxson HO, Opazo Saez A, Pare PD. Lung structure and function in cigarette smokers. Thorax. 1994 May;49(5):473-8.
24. Wright JL, Churg A. Animal models of cigarette smoke-induced COPD. Chest. 2002 Dec;122(6 Suppl):301S-6S.
25. Postnov AA, Meurrens K, Weiler H, Van Dyck D, Xu H, Terpstra P, et al. In vivo assessment of emphysema in mice by high resolution X-ray microtomography. J Microsc. 2005 Oct;220(Pt 1):70-5.